



HAL
open science

Modeling the Thermal Denaturation of the Protein–Water System in Pulses (Lentils, Beans, and Chickpeas)

Charlotte Lefèvre, Philippe Bohuon, Valérie Lullien-Pellerin, Christian Mestres

► **To cite this version:**

Charlotte Lefèvre, Philippe Bohuon, Valérie Lullien-Pellerin, Christian Mestres. Modeling the Thermal Denaturation of the Protein–Water System in Pulses (Lentils, Beans, and Chickpeas). *Journal of Agricultural and Food Chemistry*, 2022, 70 (32), pp.9980-9989. 10.1021/acs.jafc.2c03553 . hal-03748801

HAL Id: hal-03748801

<https://hal.inrae.fr/hal-03748801v1>

Submitted on 19 Jul 2023

HAL is a multi-disciplinary open access archive for the deposit and dissemination of scientific research documents, whether they are published or not. The documents may come from teaching and research institutions in France or abroad, or from public or private research centers.

L'archive ouverte pluridisciplinaire **HAL**, est destinée au dépôt et à la diffusion de documents scientifiques de niveau recherche, publiés ou non, émanant des établissements d'enseignement et de recherche français ou étrangers, des laboratoires publics ou privés.

1
2 **Modeling the thermal denaturation of the protein-**
3 **water system in pulses (lentils, beans and chickpeas)**

4
5 Charlotte Lefèvre ^a, Philippe Bohuon ^{a*}, Valérie Lullien-Pellerin ^b, Christian

6 Mestres ^{a,c}

7
8 ^a Qualisud, Université de Montpellier, Avignon Université, CIRAD, Institut Agro, IRD,
9 Université de La Réunion, 34090 Montpellier, France.

10 ^b IATE, Université de Montpellier, INRAE, Institut Agro, 34000 Montpellier, France.

11 ^c CIRAD, UMR Qualisud, F-34398 Montpellier, France.

12
13 ***Corresponding author:** Philippe Bohuon, *Institut Agro, UMR Qualisud, 1101 Av. Agropolis,*
14 *34090 Montpellier, France.* Tel: +33 4 67 87 40 81; Fax: +33 4 67 61 44 44. E-mail address:
15 philippe.bohuon@supagro.fr

18 **Abstract**

19 Thermal treatment applied during the cooking of pulses leads to denaturation and even
20 aggregation of the proteins, which may impact protein digestibility. Thermal transitions of
21 lentil, chickpea and bean proteins were studied using DSC. Protein-enriched samples were
22 obtained by dry air classification of dehulled seeds and were heated up to 160 °C, with water
23 contents ranging from 0.2 to 4 kg/kg dry basis. The DSC peaks of the resulting endotherms
24 were successfully modeled as overlapping Gaussian functions. The denaturation temperatures
25 were modeled as a function of temperature according to the Flory-Huggins theory. The
26 modeling allows to calculate the degree of protein transition for any temperature and moisture
27 condition. The denaturation diagrams reflect the different protein compositions of lentil,
28 chickpea and bean (particularly the 11S/7S globulin ratio). Chickpea proteins were more
29 thermally stable than those from lentil and bean. Proteins underwent an irreversible transition,
30 suggesting that unfolding and aggregation were coupled.

31

32

33 **Keywords**

34 Protein denaturation, DSC, Mathematical modeling, Pulses, Globulin, Peak desummation

35

36

37 1. Introduction

38 According to the FAO¹, pulses are legume crops that are harvested for their edible dry seeds
39 but are not used for oil extraction. The International Year of Pulses (2016) highlighted their
40 important nutritional benefits as part of sustainable food production targeting food security and
41 nutrition. The seeds are rich in carbohydrates including starch, as well as in proteins and dietary
42 fibers, and are a source of minerals and vitamins.² In particular, their high protein content (15-
43 30 % dry weight)³ makes pulses an excellent source of plant-based proteins for the formulation
44 of food and ingredients. However, the impact of processing on protein bioavailability and
45 digestibility is important to take into account. In particular, thermal treatment during cooking
46 leads to protein denaturation and aggregation⁴, the latter being one of the main adverse effects
47 on protein digestibility.^{5,6}

48 Inter and intra molecular bonds that stabilize the native structure of the protein are allowed to
49 break down during heating, depending on the temperature applied.⁴ This transition from a native
50 state to a more disordered arrangement is called denaturation. Pulse proteins, which are
51 oligomeric proteins with quaternary structure, undergo reversible dissociation into monomers.⁷
52 Both the tertiary and secondary structure are affected with irreversible unfolding that generally
53 remains partial.⁴ Denaturation of pulse proteins occurs between 80 °C and 100 °C in excess
54 water.⁸⁻¹⁰ This spatial reorganization leads to exposure of the reactive groups, especially the
55 hydrophobic amino acid residues embedded in the core of the native protein.⁴ As a consequence,
56 the formation of new bonds and interactions between partially unfolded peptide chains is
57 favored. The protein aggregation that follows the denaturation process results in the formation
58 of soluble or insoluble high molecular weight complexes. Protein aggregation reduces access
59 to certain essential amino acids that are specific for protease action, and that are trapped inside
60 the aggregate structures.¹¹ Heat-induced aggregation can thus impair protein digestibility of
61 cooked pulses⁶, to an even greater extent if aggregation is high.⁵ Therefore, a better

62 understanding of the denaturation-aggregation status of proteins is needed, as a function of the
63 cooking conditions to enable more accurate monitoring of the nutritional aspect. It should be
64 noted that the presence of other factors that affect digestibility such as heat-sensitive anti-
65 nutritional factors (enzymes inhibitors) also requires monitoring.

66 Previous studies on the denaturation of legume proteins mainly focused on thermal stability at
67 constant water content. However, cooking in water implies that pulses undergo hydration. The
68 water content in the seed increases from the initial value to reach equilibrium moisture.¹² Phase
69 transitions of other components of the seed, *i.e.* gelatinization of starch, also result in varying
70 hydration rates, meaning the water content in the protein pool changes during cooking.
71 Denaturation-aggregation thus needs to be described as a function of the water content. A
72 similar approach to the one developed for the modeling of gelatinization-melting of starch at
73 increasing temperature and water content¹³ should be suitable. In the present study, the phase
74 transitions of proteins were monitored using differential scanning calorimetry (DSC), a reliable
75 and convenient thermo-analytical method to study the endothermic and exothermic changes
76 associated with the denaturation and aggregation of proteins.^{14,15} To avoid the structural
77 modifications usually caused by chemical extraction reported in most studies, we chose to work
78 on protein-enriched samples obtained using a physical separation method only, *i.e.* air
79 classification. The study was focused on beans, lentils and chickpeas, which are widely
80 produced and the most consumed pulses in France.¹⁶

81

82 2. Materials and methods

83 2.1 *Raw material*

84 Green lentils (*L. culinaris*, var. Anicia), chickpeas (*C. arietinum*, var. Elvar) and navy beans
85 (*P. vulgaris*, var. Linex) were provided by Cibèle (Saint-Georges-Sur-Arnon, France), Moulin

86 Marion (Saint-Jean-sur-Veyre, France) and Cavac (La Roche-sur-Yon, France), respectively.
87 The lentils were harvested in 2017 and the chickpeas and beans in 2018. All the seeds were
88 stored in a vacuum pack at 7 °C until use.

89 2.2 *Sample preparation*

90 Protein-enriched samples were prepared by dry fractionation and air classification as described
91 in Lefèvre *et al.*¹³ Briefly, lentil seeds were dehulled by dry abrasion and residues of the hull
92 were removed by sieving through a 2-mm mesh screen. Chickpea and bean seeds were crushed
93 using a cutting mill equipped with a 8-mm sieve and residues of the hull were removed with a
94 vibrating sieve. For all pulses, the removed hulls represented 10-12% of the raw weight, and
95 the process induced 6-8% of losses. The dehulled and crushed pulses were ground into flour in
96 a high speed impact mill equipped with a pin mill. The resulting flours were separated into
97 coarse and fine fractions using an ATP air classifier (Hosokawa Alpine, Augsburg, Germany)
98 with the following optimized speeds: 6 500 rpm for lentils, 10 000 rpm for chickpeas and
99 8 000 rpm for beans. The resulting fine fractions were stored at 4 °C until use and are hereafter
100 referred to as protein-enriched samples.

101 2.3 *Sample characterization*

102 Water content of the protein-enriched samples was calculated on a wet basis by drying 5 g of
103 each sample for 2 h at 132 °C (± 2 °C) using the NF EN ISO 712 standard method (2010).
104 Starch content was measured using the enzymatic procedure of Holm *et al.*¹⁷ Protein content
105 was measured using the Kjeldhal method according to NF EN ISO 20483, with 5.4 as nitrogen
106 conversion factor.¹⁸ Lipid content was measured using the gravimetric ether extraction method
107 according to AOAC 2003.05.¹⁹ Soluble and insoluble fibers were measured using a TDF
108 Analyzer (Ankom, Macedon, USA) according to AOAC 2011.25 and AACC 32-50.01.²⁰
109 Phytates were extracted according to a published method²¹ with some modifications. A 100 mg-

110 sample was added to a Pyrex vial with 5 mL of 0.5 M HCl. The capped vial was heated under
111 stirring for 6 min in boiling water and then centrifuged for 20 min at 4 500 g. The supernatant
112 was recovered and filtered through a 0.2 μm syringe filter (Acrodisc) and 0.5 M NaOH was
113 added for neutralization and the solution was then diluted (1:10). Phytic acid content was
114 measured by high performance ion chromatography (HPIC) using an ICS-2500 Dionex
115 chromatograph (Sunnyvale, CA, USA). Fiber and phytate measurements were made in
116 triplicate and all other measurements were made in duplicate.

117 2.4 *Differential scanning calorimetry*

118 Thermal denaturation of proteins was studied by DSC as described in Lefèvre *et al.*¹³ Briefly,
119 a Perkin DSC 8500 (Perkin Elmer, Norwalk, USA) was calibrated using indium as standard.
120 Protein-enriched samples and deionized water were weighed in stainless steel pans to obtain a
121 water content X ranging from 0.2 to 4 kg kg⁻¹ dry basis (db). This range covers the progressive
122 hydration of proteins while the pulses are cooking. The pans were heated from 20 °C to 160 °C
123 at a rate of 10 °C/min, using an empty sealed pan as reference. All measurements were
124 duplicated. A blank thermogram (empty pans in both reference and sample ovens) was recorded
125 daily. The heat flow (mW) of the sample pans minus the variation in the heat flow of the blank
126 during heating was recorded using Pyris Thermal Analysis Software (Perkin Elmer, Norwalk,
127 USA). Table 1 lists the experimental conditions applied for the different water contents. In the
128 study conditions (*i.e.* at $T \leq 160$ °C), the lowest water content to be able to detect a complete
129 DSC signal was 0.2, 0.3 and 0.4 kg kg⁻¹ db, for beans, lentils and chickpeas, respectively. When
130 the heat flows were similar for close water contents, fewer intermediate water contents were
131 used. In addition, double scans were performed with an intermediate water content of
132 0.8 kg kg⁻¹ db. Samples were heated from 20 °C to 80 °C, 110 °C or 160 °C at a rate of
133 10 °C/min, then cooled to 20 °C and heated a second time from 20 °C to 160 °C at a rate of
134 10 °C/min.

135 **[Insert Table 1 here]**

136 2.5 *Modeling the protein denaturation diagram*

137 DSC thermograms record heat flow (φ) as a function of temperature (T) at each water content.
138 Phase transitions of the sample components result in peaks in the endotherm. The DSC
139 thermograms obtained from the protein-enriched samples are discussed as if the peaks were
140 only due to the phase transition of proteins. This hypothesis will be confirmed in the results
141 part.

142 2.5.1 *Modeling the DSC peaks*

143 Thermal denaturation of the protein-enriched samples resulted in single or double peaks in the
144 DSC signal depending on the variety of the pulse concerned. The shape of all the endotherms
145 depended on water content. Therefore, heat flows were analyzed according to the desummation
146 procedure described in Lefèvre *et al.*¹³ on pulse starches. First, baseline subtraction and non-
147 dimensionalization were performed on heat flow values in all pulses. In the lentil and chickpea
148 samples, the heat flow was composed of two roughly overlapping endotherms depending on
149 the water content, termed P1 and P2. The dimensionless heat flows ($\bar{\varphi}$) were fitted to a sum of
150 two Gaussian functions ($i = P1$ or $P2$) as follows:

151
$$\bar{\varphi} = \sum_{i=P1,P2} \frac{\beta_i}{\Delta T_i \sqrt{2\pi}} \exp\left(-\frac{1}{2} \left(\frac{T-T_i}{\Delta T_i}\right)^2\right) \quad (1)$$

152 where T_i (°C) is the temperature at maximum peak i ; ΔT_i (°C) controls the width of the peak i
153 and is related to the full width at half maximum (FWHM) of the peak i according to
154 $2\sqrt{2 \ln(2)} \times \Delta T_i = \text{FWHM}$; β_i is the dimensionless area of peak i . Therefore:

155
$$\int_{-\infty}^{\infty} \bar{\varphi} = \beta_{P1} + \beta_{P2} = 1 \quad (2)$$

156 In bean, the heat flow had a single endotherm ($i = P1$) irrespective of water content, so $\beta_{P1} = 1$.
 157 Eq. (1) was similar to the equation used previously for modeling starch conversion heat flow¹³
 158 which was composed of overlapping gelatinization and melting peaks. The parameters from
 159 Eq. (1) depend on the water content X in the samples.

160 2.5.2 Peak temperature

161 The temperature at maximum peak T_i ($^{\circ}\text{C}$) is the denaturation temperature of the proteins
 162 responsible for transition i ($i = P1$ or $P2$). The Flory–Huggins equation²² was used to describe
 163 the relation between T_i and the volume fraction of the water (ϕ) in the protein-water mixture:

$$164 \quad \frac{1}{T_i} - \frac{1}{T_{i,0}} = \frac{R}{\Delta h_{i,0}} \frac{v_a}{v_w} (\phi - \chi_i \phi^2) \quad (3)$$

165 where $\Delta h_{i,0}$ (J mol^{-1}) is the change in the molar enthalpy of denaturation per repeating unit
 166 (amino acid); v_a / v_w is the ratio of the molar volume of the repeating unit
 167 ($v_a = 74.5 \times 10^{-6} \text{ m}^3 \text{ mol}^{-1}$)²³ to the molar volume of the water ($v_w = 18.1 \times 10^{-6} \text{ m}^3 \text{ mol}^{-1}$) and,
 168 therefore, $v_a / v_w = 4.1$; R is the gas constant ($8.31 \text{ J mol}^{-1} \text{ K}^{-1}$); $T_{i,0}$ (K) is the denaturation
 169 temperature of the pure polymer and χ_i is the Flory interaction parameter. To calculate ϕ , the
 170 density of water was taken to be 1000 kg m^{-3} and the density of protein was attributed an
 171 average value of 1350 kg m^{-3} .²⁴ Therefore, ϕ ($\text{m}^3 \text{ m}^{-3}$) was expressed as a function of water
 172 content X :

$$173 \quad \frac{1}{\phi} = 1 + \frac{x_p^{db}}{1.35X} \quad (4)$$

174 where x_p^{db} ($\text{kg kg}^{-1} \text{ db}$) is the mass fraction of protein in the protein-enriched samples.

175 2.5.3 Peak width

176 The width-related parameter ΔT_i represents the cooperativity of protein unfolding process and
 177 the presence of multiple protein domains with heterogeneous thermal stabilities.^{4,25} ΔT_i was
 178 likely to decrease as a function of water content. The following empirical relation was used to
 179 describe ΔT_i as a function of X :

$$180 \quad \Delta T_i = \Delta T_{i,\infty} + (\Delta T_{i,0} - \Delta T_{i,\infty}) \exp\left(-\frac{X}{\gamma_i}\right) \quad (5)$$

181 where $\Delta T_{i,0}$ (°C) and $\Delta T_{i,\infty}$ (°C) are the values for ΔT_i , with zero and excess water contents,
 182 respectively; γ_i is the rate parameter of decrease for the two correlations.

183 2.5.4 Amplitude of the peak area

184 The effect of water content on the relative peak areas β_i was also investigated. With increasing
 185 water content, β_{P1} was likely to decrease. The following empirical equation was used to
 186 describe this relation for lentil and chickpea:

$$187 \quad \beta_{P1} = \beta_{P1,\infty} + (\beta_{P1,0} - \beta_{P1,\infty}) \exp(-X) \quad (6a)$$

188 where $\beta_{P1,0}$ and $\beta_{P1,\infty}$ are the dimensionless area of the first peak, with zero and excess water
 189 contents, respectively. β_{P2} was calculated by combining Eq. (2) and Eq. (6a) as follows:

$$190 \quad \beta_{P2} = 1 - \left[\beta_{P1,\infty} + (\beta_{P1,0} - \beta_{P1,\infty}) \exp(-X) \right] \quad (6b)$$

191 2.5.5 Degree of protein denaturation

192 The degree of protein denaturation τ was defined for any temperature T and water content X
 193 as the ratio between the change in enthalpy calculated from the beginning of the first peak to T ,
 194 and the change in the whole enthalpy from the beginning of the first peak to the end of the
 195 second peak (Eq. (7a)). Denaturation refers to the global transition of proteins, which includes
 196 unfolding and potential aggregation.

197
$$\tau = \int_0^T \bar{\varphi}(T, X) dT \bigg/ \int_0^\infty \bar{\varphi}(T, X) dT \quad (7a)$$

198 Using the error function to calculate integral Gaussian functions, Eq. (7a) becomes Eq. (7b) for
 199 lentil and chickpea (with $i = P1$ and $P2$) and for bean (with only $i = P1$).

200
$$\tau = \sum_{i=P1,P2} \beta_i \times \frac{1}{2} \left(1 + \operatorname{erf} \left(\frac{T - T_i}{\Delta T_i \sqrt{2}} \right) \right) \quad (7b)$$

201 Finally, isovalue lines of the degree of protein denaturation τ were represented as a
 202 temperature T versus water content X diagram.

203 *2.5.6 Identification of parameters*

204 The modeling of protein denaturation diagram involves 9 parameters for lentil ($T_{i,0}$, $\Delta h_{i,0}$, χ_i ,
 205 ΔT_i , β_{P1}), 13 parameters for chickpea ($T_{i,0}$, $\Delta h_{i,0}$, χ_i , $\Delta T_{i,0}$, $\Delta T_{i,\infty}$, γ_{P2} , $\beta_{P1,0}$ and $\beta_{P1,\infty}$) and
 206 4 parameters for bean ($T_{P1,0}$, $\Delta h_{P1,0}$, χ_{P1} , ΔT_{P1}), with $i = P1$ or $P2$. The overall procedure¹³ was
 207 used to identify all the parameters. At the same fitting session, all dimensionless heat flow
 208 thermograms were fitted to the model combining Eq. (3), (5) and (6a) in Eq. (1). The curve
 209 fitting toolbox (Matlab software, version R2019b, The MathWorks Inc., Natick, USA) with the
 210 Levenberg-Marquardt algorithm was used as a solver.

211 *2.5.7 Statistical methods*

212 All parameter values presented in this study are given with a 95% confidence interval. The root
 213 mean square error (RMSE) was calculated between experimental and predicted dimensionless
 214 heat flows for all the experimental conditions.

215

216 **3. Results and Discussion**

217 *3.1 Characterization of the samples*

218 **[Insert Table 2 here]**

219 The chemical composition of the protein-enriched fractions obtained after dry fractionation and
220 air classification are listed in Table 2. Proteins were the main component in the fine fractions,
221 with x_p^{db} ranging from 38.2% of db weight for chickpea to 55.8% db for lentil. These values
222 are in good agreement with protein concentration range of 40-60% db reported in literature for
223 air-classification on pulse flours.²⁶⁻²⁸ Protein contents of the dehulled seeds were 24.1% db,
224 19.3% db and 23.2% db in lentil, chickpea and bean, respectively. The dry air-classification
225 process can thus be considered as an efficient physical method to produce protein-enriched
226 samples while avoiding the structural modifications that may occur with chemical extraction.
227 Tyler *et al.*²⁷ already reported good protein separation efficiency using air-classification,
228 particularly for green lentil and navy bean. Insoluble dietary fibers (IDF) were the second
229 component in the protein-enriched samples, ranging from 11.1% db for lentil to 18.5% db for
230 chickpea. Other components listed in Table 2 represented all together 25-37% db of the samples
231 and between 2 and 11% db each. The interactions between proteins and those non-proteins
232 components may affect the thermal stability of proteins²⁹ and the water repartition due to the
233 competition for available water³⁰. These interactions may impact the denaturation temperature
234 of proteins and were intrinsic to the protein-enriched samples studied here. There have not been
235 investigated further.

236 *3.2 DSC characteristics of the protein-enriched fractions*

237 **[Insert Fig. 1 here]**

238 **[Insert Fig. 2 here]**

239 **[Insert Table 3 here]**

240 For each pulse, Fig. 1 presents a selection of three DSC thermograms at $X=0.4$, 1.0 and
241 2.0 kg kg^{-1} db. All transition peaks were observed above 60 °C, so the temperature range of
242 interest was between 60 and 160 °C. According to the protein enrichment of the fine fractions

243 after air-classification in comparison with other components (Table 2), we confirmed the
244 hypothesis that the DSC thermograms were mainly due to protein denaturation. Indeed, the
245 second main component of the samples, IDF, underwent no thermal transition below 200 °C.³¹
246 Denaturation of phytates and alpha-galactosides also occurred at temperatures exceeding the
247 conditions of the study, whereas the melting point of lipids was lower than the temperature
248 range of interest. Thus, only the gelatinization of residual starch could lead to additional DSC
249 peaks in the temperature range of interest. However, the starch content was less than 6% db in
250 all samples, resulting in a low contribution to the total enthalpy of the observed transition. The
251 DSC peak were thus mainly attributed to the phase transitions of proteins.

252 The experiments revealed that the thermal behavior of proteins depended on both the water
253 content and the type of pulse (Fig. 1). The DSC thermograms for lentils showed two roughly
254 overlapping peaks P1 and P2, depending on the moisture content of the sample. With lower
255 water content (i.e. $X \leq 2 \text{ kg kg}^{-1} \text{ db}$), a biphasic endotherm was observed. With excess water, a
256 single broad peak was observed, suggesting that both peaks are merged as modeled by the
257 Gaussian functions (Fig. 1c). The endotherm for chickpea had two distinct peaks, P1 and P2,
258 regardless of the water content. The shape and size of the peaks changed with the moisture
259 content. The endotherm for bean had a single peak, P1, of constant size and shape, regardless
260 of the water content. All DSC thermograms were successfully modeled as shown by the low
261 RMSE between experimental and predicted heat flows (Fig. 1). The parameters presented in
262 Table 3 had low confidence intervals, which allows accurate modeling of experimental data.
263 Modeling is particularly useful to understand the superposition of P1 and P2 endotherms.

264 The multiple or overlapping peaks observed by DSC showed that the thermal stability of the
265 proteins varied. This is linked to the different protein fractions in the seed. The main proteins
266 in pulses are globulins and albumins in varying proportions depending on the species and
267 variety of the pulse concerned.^{3,32} Almost all pulses contain two main types of globulins with

268 sedimentation coefficients around 7S and 11S called vicilin and legumin, respectively.^{33,34} The
269 temperature, shape and size of the denaturation endotherms presented in Fig. 1 were thus
270 determined mainly by the thermal denaturation of 7S and 11S globulins. Vicilin has a trimeric
271 structure stabilized by hydrophobic interactions, electrostatic and hydrogen bonds. Legumin
272 has a quaternary structure made of three dimers held together by non-covalent bonds. In each
273 dimer, acidic and basic subunits are associated with disulfide bridges.⁷ The covalent bonds give
274 legumin higher thermal stability than vicilin, because more energy is needed to break the
275 bonds.³⁵ In excess water, 7S and 11S globulins unfold at 80-85 °C and 90-100 °C,
276 respectively.^{10,36} In lentil, endotherms P1 and P2 were attributed to the denaturation of 7S and
277 11S globulin, respectively, with peak temperatures at 83 °C and 91 °C (with $X = 3 \text{ kg kg}^{-1} \text{ db}$).
278 $\beta_{P1,0}$ and $\beta_{P1,\infty}$ did not differ significantly in lentils, β_{P1} thus remained constant and equal to
279 0.65 irrespective of the water content (Table 3). This value suggests that the P1 transition was
280 slightly predominant than to P2 transition. In chickpea, endotherms P1 and P2 were again
281 attributed to the successive denaturation of 7S and 11S globulin, respectively, with peak
282 temperatures at 83 °C and 103 °C (with $X = 3 \text{ kg kg}^{-1} \text{ db}$). β_{P1} was lower than 0.5, except at the
283 lowest water contents ($X \leq 0.5 \text{ kg kg}^{-1} \text{ db}$). This trend suggests that the legumin transition was
284 predominant in chickpea. This result is in good agreement with the high 11S/7S ratio commonly
285 reported for several chickpea species.³⁷⁻³⁹ The decreasing function for β_{P1} (Fig. 2e) suggests
286 that part of the 7S globulin was solubilized without denaturation with increasing water content.
287 This hypothesis is consistent with the decrease in total enthalpy of phase transition observed
288 before non-dimensionalization (from 21 to 10 J g⁻¹ protein when X increased from 0.4 to
289 1 kg kg⁻¹ db). In some cases, denaturation peaks of vicilin and legumin in chickpea have been
290 reported to overlap.^{10,37} In bean, the single peak P1 at 92 °C (with $X = 3 \text{ kg kg}^{-1} \text{ db}$) was
291 attributed to the predominant vicilin fraction, as already suggested in several bean
292 varieties.^{9,14,40} The diversity of DSC signals between lentil, chickpea, and bean clearly reflects

293 the variations in the 11S/7S ratio between pulses, as already reported.^{26,41} In this sense, DSC
294 analysis can be used to rapidly determine globulin ratios when determination using
295 chromatography and electrophoresis on protein isolates is not possible.

296 *3.3 Modeling of peak width and temperature*

297 No significant difference was observed between $\Delta T_{i,0}$ (°C) and $\Delta T_{i,\infty}$ in lentil and bean, the
298 peak widths ΔT_i were thus constant and equal to $\Delta T_{i,\infty}$ (Table 3). This low value (3-4 °C)
299 reflected highly cooperative unfolding for vicilin and legumin, irrespective of the water
300 content.²⁵ In chickpea, ΔT_i decreased with a reduction in water content, as shown by the
301 decreasing exponential law (Fig. 2 and Table 3). The progressive sharpening of both P1 and P2
302 peaks showed that increasing moisture led to a more cooperative denaturation of chickpea
303 vicilin and legumin.⁴ The heterogeneous composition of the protein-enriched samples may also
304 play a role in the DSC characteristics. The lower protein content in chickpea than in lentil and
305 bean (Table 2) may lead to a broader and more water-sensitive endotherm in the DSC
306 thermogram due to the lower protein purity and hence, possible interaction with residual
307 components, in particular with the higher IDF content.²⁹

308 The denaturation temperatures T_i of lentil, bean and chickpea proteins decreased with an
309 increase in water volume fraction (Fig. 2). Temperatures were modeled using the Flory-
310 Huggins theory for a polymer in solution (Eq. 3). The coefficient of determination (R^2) was
311 0.98-0.99 for T_{p1} and 0.96-0.99 for T_{p2} . The fitting strength shows that this model fits both 7S
312 and 11S protein denaturation in all pulses studied. Concerning the P1 transition, the
313 denaturation temperatures of pure polymer were similar for lentil and bean, with a $T_{p1,0}$ value
314 of 165.2 °C and 166.2 °C, respectively. $T_{p1,0}$ was 30 °C higher for chickpea. Again for the P2
315 transition, $T_{p2,0}$ was 20 °C higher for chickpea legumin compared to lentil legumin (Table 3).

316 The denaturation temperatures of pure protein varied more between pulses than the denaturation
317 temperatures of gelatinization and melting of pure starch, obtained with the same Flory-
318 Huggins model.¹³ The change in molar enthalpy of denaturation $\Delta h_{i,0}$ ranged from 41.2 kJ mol⁻¹
319 ¹ to 65.8 kJ mol⁻¹ for vicilin and from 41.9 to 45.1 kJ mol⁻¹ for legumin (Table 3). These
320 enthalpies were higher than the change in molar enthalpy of gelatinization and melting of
321 starch.¹³ The Flory interaction parameter χ_i was low (0-0.14) compared to the range 0.48-0.51
322 previously reported for cereal, potato or pulse starches.^{13,42-44} These values suggests that the
323 interactions between water and proteins were low.⁴⁴ To conclude, all the values determined for
324 Flory-Huggins parameters ($T_{i,0}$, $\Delta h_{i,0}$, χ_i) differ from those previously obtained for starch
325 gelatinization and melting modeling. The Flory-Huggins theory is thus an accurate and useful
326 tool for predicting the impact of moisture on the denaturation temperatures of pulse proteins.

327 *3.4 Relevance of the predicted denaturation temperatures*

328 Denaturation temperatures T_i modeled using the Flory-Huggins parameters described above
329 were consistent with denaturation temperatures already reported for lentil, chickpea and bean
330 proteins. For lentil in excess water ($X = 10$ kg kg⁻¹ db), two overlapping peaks were found at
331 77.9 °C and 83.7 °C, respectively. At the same water content and also in green lentil proteins,
332 Barbana and Boye³⁶ observed a similar result with a broad peak at 79.6 °C. The denaturation
333 temperatures of green lentil proteins were lower than those of red lentil proteins, which have
334 been reported to range from 87 °C in excess water to 123 °C with limited water.^{36,45} For
335 chickpea, T_{p1} and T_{p2} were predicted to be 83.3-84.9 °C and 101.9-103.6 °C, respectively, when
336 X ranged between 3 and 4 kg kg⁻¹ db. These values are in good agreement with the denaturation
337 temperatures of chickpea proteins reported in previous studies for the same range of water
338 content.⁴⁶⁻⁴⁸ These authors reported broad peaks ranging from 85 °C to 100 °C, depending on
339 the varieties and on the extraction methods used. Our results differ slightly from the two peaks

340 observed by Chang *et al.*³⁷ at 79.3 °C and 96.3 °C. At higher water content ($X = 9 \text{ kg kg}^{-1} \text{ db}$),
341 Withana-Gamage *et al.*¹⁰ reported a vicilin transition at 80-85 °C depending on the variety of
342 chickpea, which is similar to our T_{p1} at 80.5 °C. The same authors reported that the legumin
343 transition occurred at 89.2-93.2 °C, which is lower than our T_{p2} predicted at 99.0 °C. For bean
344 in excess water ($X = 10 \text{ kg kg}^{-1} \text{ db}$), we found a single peak at 87.1 °C. This temperature was
345 slightly lower than the peak temperature of 90.6 °C reported by Rui *et al.*⁹ in white bean, the
346 same variety as the navy bean we used in the present study. Yin *et al.*⁴⁰ and Law *et al.*⁴⁹ also
347 reported higher peak temperatures for red bean and rice bean, respectively (92.5 °C and 91.9 °C,
348 respectively). Meng and Ma¹⁴ observed a major peak at 86.4 °C close to our result, and a
349 shoulder at 92.2 °C for red bean globulin, at the same water content. Their measurements on
350 fractionated fractions showed that the DSC signal could be split into a biphasic endotherm for
351 7S vicilin (peaks at 88 °C and 94 °C) due to non-glycosylated and glycosylated subunits, and a
352 minor endotherm for 11S legumin (peak at 89.5 °C), overlapping the first one. In the present
353 study, it is possible to hypothesize that a peak at a higher temperature than T_{p1} but with a lower
354 amplitude may be hidden under P1 endotherm, corresponding with the denaturation of residual
355 11S legumin.

356 The denaturation temperature of proteins can differ considerably among pulse species, and also
357 between varieties of the same species. In this study, the denaturation temperature of green lentil
358 and navy bean proteins was lower than the denaturation temperatures reported for red lentil and
359 for red and rice beans, respectively. A difference of up to 10 °C has been reported among the
360 denaturation temperatures of proteins in different bean varieties.^{9,49} This variability is linked to
361 the different proportions of storage proteins.³² It is important to underline that the DSC
362 characteristics are also affected by environmental and processing conditions, and protein
363 extraction methods.^{15,36,45} Studying pure vicilin and legumin fractions or a globulin mixture
364 may also lead to slight variations in the denaturation temperatures.^{14,15,37} The purity degree of

365 the protein sample is important because the thermal stability of proteins may be affected by
366 interactions between protein and non-protein components.²⁹ All these factors can explain the
367 variations in denaturation temperatures, number and shape of DSC peak between studies on a
368 similar pulse cultivar.

369 3.5 Thermal aggregation of proteins

370 **[Insert Fig. 3 here]**

371 Double scans were performed in order to determine if the observed transitions were reversible,
372 *i.e.* still observable on the DSC signal after a preheating treatment. The first heating treatments
373 are hereafter referred to as preheating. The DSC signals of the second heating treatments are
374 presented in Fig. 3 and showed that a peak disappears when the temperature of the preheating
375 exceeds the temperature of the transition considered. For all pulses, a preheat treatment to 80 °C
376 did not damage the protein, since the DSC thermograms were similar to the control. This is
377 consistent with the higher denaturation temperatures described above. When lentil and chickpea
378 samples were preheated to 110 °C (Fig. 3a and b), only one transition was observed at a
379 temperature corresponding to the P2 transition of the untreated sample (115-120 °C). This
380 means that the vicilin transition P1 was no longer detected, while the legumin peak P2 was still
381 observed. In addition, the legumin peak was no longer detected when the sample was preheated
382 to 160 °C. These results confirm that 11S globulin is more thermally stable than 7S globulin.
383 Also in bean, vicilin was irreversibly damaged at 110 °C (Fig. 3c). In conclusion, both types of
384 protein were irreversibly damaged when the thermal treatment exceeded their denaturation
385 temperature. Ricci *et al.*²⁹ also observed irreversible denaturation process using DSC. The
386 authors reported additional reversible glass transition for lentil, bean and chickpea ($X = 0.15$
387 kg kg^{-1}) ranging from 150 to 170 °C. The differences in water content, heating temperatures,
388 protein purity and pulse variety may explain why a similar glass transition was not observed on
389 the DSC thermograms in Fig. 3.

390 The irreversibility of the transition suggests that thermal denaturation involves both unfolding
391 of the structure and aggregation between protein chains.^{10,11} Partially denatured proteins may
392 form a soluble and insoluble complex with new interactions. German *et al.*⁸ showed that the
393 dissociation of 11S purified soy proteins during heating was followed by aggregation of the
394 released basic subunits into insoluble complexes. In the presence of 7S proteins, basic 11S
395 subunits and 7S subunits can form soluble complexes. Denaturation and aggregation seemed to
396 be coupled in the present study, or at least not separable using DSC analysis. Sirtori *et al.*³⁵ also
397 reported irreversible denaturation of pea globulins. These authors reported that the vicilin peak
398 disappeared from the DSC thermogram when samples were pre-heated to 200 °C, or heated at
399 100 °C for a long time (120-300 min). The 11S peak was visible in all conditions, even after
400 harsh treatment at 200 °C, but its detergent solubility decreased.

401 3.6 Modeling the denaturation diagram of proteins

402 **[Insert here] Fig. 4.**

403 The results obtained with desummation modeling allowed us to calculate the degree of protein
404 denaturation (including unfolding and aggregation) for any temperature T and water content X .
405 Some isovalue lines of degree of protein denaturation are presented as a T versus X diagram in
406 Fig. 4. The differences we observed in the denaturation temperatures between the three pulses,
407 related to their respective protein composition, are still visible in the diagram. The higher
408 11S/7S ratio for chickpea led to isovalue lines of denaturation degree at higher temperatures
409 than for bean and lentil proteins. For example, to achieve 99% protein denaturation at
410 $X = 4 \text{ kg kg}^{-1} \text{ db}$, lentil and bean should be heated to 96-98 °C while chickpea should be heated
411 to 111 °C. The fact that the thermal behavior depends on the species and variety of pulse means
412 that extrapolating this diagram to other legumes will be tricky, in contrast to extrapolating the
413 starch gelatinization diagram.¹³ The specific denaturation characteristics of each pulse need to
414 be known to accurately predict the denaturation state of the proteins.

415 In addition, some studies^{35,50} demonstrated that the length of the thermal treatment and the
416 moisture conditions have an effect on the degree of denaturation of pulse proteins. This result
417 suggests that protein denaturation-aggregation should be considered as a kinetic process. From
418 this point of view, our diagram represents a short heating time (8 minutes heating at between
419 80 °C and 160 °C). With longer heating times, the final diagram would probably be different.

420

421 To conclude, the DSC experiments on protein-enriched fractions of pulses and the desummation
422 method of the thermograms were suitable for modeling the thermal denaturation of pulse
423 proteins. The temperature, shape and size of the DSC peaks were consistent with the protein
424 composition of each pulse, in particular the 11S/7S globulin ratio. The single transition
425 observed for bean was characteristic of 7S vicilin denaturation, which is the main globulin in
426 this pulse. However, an endotherm with two transitions was observed for chickpea and lentil.
427 Its thermal characteristics are in good agreement with the denaturation of 7S vicilin and then
428 11S legumin at higher temperatures. Irreversible denaturation of both protein types was
429 observed, suggesting that unfolding and aggregation were coupled under the heating conditions
430 used in the study. The three obtained diagrams of protein denaturation enable monitoring of the
431 phase status of lentil, chickpea and bean proteins, in different T and X conditions. However, the
432 diagrams cannot be used to generalize denaturation temperature ranges to all cultivars and has
433 to be studied with a case-by-case approach as composition may vary.

434 Since the unfolding and aggregation caused by processing, such as heating, modifies the
435 functionality and nutritional quality of pulse proteins, denaturation diagrams are key parameters
436 to improve the cooking process of pulses. The next step in this work will be to combine the
437 phase transition models for starch and for proteins to provide a model of physicochemical
438 changes at the seed scale. However, the present results should be interpreted with caution, as
439 the proteins may behave differently when purified or mixed with other components of the seeds.

440 **Abbreviations used**

db	Dry basis
DSC	Differential scanning calorimetry
FWHM	Full width at half maximum (°C)
P1	First peak of the DSC thermogram
P2	Second peak of the DSC thermogram
R	Gas constant ($\text{J mol}^{-1} \text{K}^{-1}$)
RMSE	Root mean square error
T	Temperature (°C)
T_i	Temperature at maximum peak i (°C)
X	Water content (kg kg^{-1} dry basis)
x_p^{db}	Mass fraction of protein (kg kg^{-1} dry basis)

Greek symbols

β_i	Dimensionless area of peak i
$\beta_{P1,0}$	Dimensionless area of first peak (P1) when water content is zero
$\beta_{P1,\infty}$	Dimensionless area of first peak (P1) in excess water
$\Delta h_{i,0}$	Change in molar enthalpy of transition i per repeating unit (J mol^{-1})
ΔT_i	Parameter related to the width of peak i (°C)
$\Delta T_{i,0}$	Parameter related to the width of peak i when water content is zero (°C)
$\Delta T_{i,\infty}$	Parameter related to the width of peak i in excess water (°C)
v_a	Molar volume of repeating unit amino acid ($\text{m}^3 \text{mol}^{-1}$)
v_w	Molar volume of water ($\text{m}^3 \text{mol}^{-1}$)
τ	Degree of protein denaturation
φ	Heat flow (W)
$\bar{\varphi}$	Normalized dimensionless heat flow
ϕ	Volume fraction of water in protein-water mixture ($\text{m}^3 \text{m}^{-3}$)
χ_i	Flory interaction parameter for i transition

442 **Acknowledgements**

443 We thank G. Maraval, INRAE (UMR IATE) for his help with isolation of the protein-enriched
444 fraction and C. Mouquet-Rivier, C. Picq, I. Rochette and C. Vernière, IRD (UMR QUALISUD)
445 for fiber and phytate measurements. The research presented in this paper was supported by the
446 Proveggas Project (22nd Inter-ministerial Fund).

447 **References**

- 448 (1) FAO (Food and Agricultural Organization). *Definition and classification of*
449 *commodities: 4. Pulses and derived products.*
450 <https://www.fao.org/waicent/faoinfo/economic/faodef/fdef04e.htm#4.01> (accessed
451 2022-04-25).
- 452 (2) Roy, F.; Boye, J. I.; Simpson, B. K. Bioactive Proteins and Peptides in Pulse Crops: Pea,
453 Chickpea and Lentil. *Food Res. Int.* **2010**, *43* (2), 432–442.
454 <https://doi.org/10.1016/j.foodres.2009.09.002>.
- 455 (3) Avezum, L.; Rondet, E.; Mestres, C.; Achir, N.; Madode, Y.; Gibert, O.; Lefevre, C.;
456 Hemery, Y.; Verdeil, J.-L.; Rajjou, L. Improving the Nutritional Quality of Pulses via
457 Germination. *Food Rev. Int.* **2022**, 1–34.
458 <https://doi.org/10.1080/87559129.2022.2063329>.
- 459 (4) Boye, J. I.; Ma, C.-Y.; Harwalkar, V. R. Thermal Denaturation and Coagulation of
460 Proteins. In *Food Proteins and their Applications*; CRC Press: Boca Raton, 1997; pp 25–
461 56.
- 462 (5) Tang, C.-H.; Chen, L.; Ma, C.-Y. Thermal Aggregation, Amino Acid Composition and
463 in Vitro Digestibility of Vicilin-Rich Protein Isolates from Three Phaseolus Legumes: A
464 Comparative Study. *Food Chem.* **2009**, *113* (4), 957–963.
465 <https://doi.org/10.1016/j.foodchem.2008.08.038>.
- 466 (6) Carbonaro, M.; Grant, G.; Cappelloni, M. Heat-Induced Denaturation Impairs
467 Digestibility of Legume (Phaseolus Vulgaris L and Vicia Faba L) 7S and 11S Globulins
468 in the Small Intestine of Rat. *J. Sci. Food Agric.* **2005**, *85* (1), 65–72.
469 <https://doi.org/10.1002/jsfa.1940>.
- 470 (7) Carbonaro, M.; Maselli, P.; Nucara, A. Structural Aspects of Legume Proteins and
471 Nutraceutical Properties. *Food Res. Int.* **2015**, *76*, 19–30.
472 <https://doi.org/10.1016/j.foodres.2014.11.007>.
- 473 (8) German, B.; Damodaran, S.; Kinsella, J. E. Thermal Dissociation and Association
474 Behaviour of Soy Proteins. *J. Agric. Food Chem.* **1982**, *30* (5), 807–811.
- 475 (9) Rui, X.; Boye, J. I.; Ribereau, S.; Simpson, B. K.; Prasher, S. O. Comparative Study of
476 the Composition and Thermal Properties of Protein Isolates Prepared from Nine
477 Phaseolus Vulgaris Legume Varieties. *Food Res. Int.* **2011**, *44* (8), 2497–2504.
478 <https://doi.org/10.1016/j.foodres.2011.01.008>.
- 479 (10) Withana-Gamage, T. S.; Wanasundara, J. P.; Pietrasik, Z.; Shand, P. J. Physicochemical,
480 Thermal and Functional Characterisation of Protein Isolates from Kabuli and Desi
481 Chickpea (Cicer Arietinum L.): A Comparative Study with Soy (Glycine Max) and Pea
482 (Pisum Sativum L.). *J. Sci. Food Agric.* **2011**, *91* (6), 1022–1031.
483 <https://doi.org/10.1002/jsfa.4277>.
- 484 (11) Carbonaro, M.; Cappelloni, M.; Nicoli, S.; Lucarini, M.; Carnovale, E.
485 Solubility–Digestibility Relationship of Legume Proteins. *J. Agric. Food Chem.* **1997**,
486 *45* (9), 3387–3394. <https://doi.org/10.1021/jf970070y>.

- 487 (12) Ibarz, A.; Augusto, P. E. D. Describing the Food Sigmoidal Behavior During Hydration
488 Based on a Second-Order Autocatalytic Kinetic. *Dry. Technol.* **2015**, *33* (3), 315–321.
489 <https://doi.org/10.1080/07373937.2014.949737>.
- 490 (13) Lefèvre, C.; Bohuon, P.; Akissoé, L.; Ollier, L.; Matignon, B.; Mestres, C. Modeling the
491 Gelatinization-Melting Transition of the Starch-Water System in Pulses (Lentil, Bean
492 and Chickpea). *Carbohydr. Polym.* **2021**, *264*, 117983.
493 <https://doi.org/10.1016/j.carbpol.2021.117983>.
- 494 (14) Meng, G.-T.; Ma, C.-Y. Thermal Properties of Phaseolus Angularis (Red Bean)
495 Globulin. *Food Chem.* **2001**, *73* (4), 453–460. [https://doi.org/10.1016/S0308-](https://doi.org/10.1016/S0308-8146(00)00329-0)
496 [8146\(00\)00329-0](https://doi.org/10.1016/S0308-8146(00)00329-0).
- 497 (15) Wright, D. J.; Boulter, D. Differential Scanning Calorimetric Study of Meals and
498 Constituents of Some Food Grain Legumes. *J. Sci. Food Agric.* **1980**, *31* (12), 1231–
499 1241. <https://doi.org/10.1002/jsfa.2740311203>.
- 500 (16) Margier, M.; Georgé, S.; Hafnaoui, N.; Remond, D.; Nowicki, M.; Du Chaffaut, L.;
501 Amiot, M.-J.; Reboul, E. Nutritional Composition and Bioactive Content of Legumes:
502 Characterization of Pulses Frequently Consumed in France and Effect of the Cooking
503 Method. *Nutrients* **2018**, *10* (11), 1668. <https://doi.org/10.3390/nu10111668>.
- 504 (17) Holm, J.; Björck, I.; Drews, A.; Asp, N.-G. A Rapid Method for the Analysis of Starch.
505 *Starch - Stärke* **1986**, *38* (7), 224–226. <https://doi.org/10.1002/star.19860380704>.
- 506 (18) Mariotti, F.; Tomé, D.; Mirand, P. P. Converting Nitrogen into Protein—Beyond 6.25
507 and Jones’ Factors. *Crit. Rev. Food Sci. Nutr.* **2008**, *48* (2), 177–184.
508 <https://doi.org/10.1080/10408390701279749>.
- 509 (19) Thiex, N. J.; Anderson, S.; Gildemeister, B. Crude Fat, Diethyl Ether Extraction, in Feed,
510 Cereal Grain, and Forage (Randall/Soxtec/Submersion Method): Collaborative Study. *J.*
511 *AOAC Int.* **2003**, *86* (5), 888–898. <https://doi.org/10.1093/jaoac/86.5.888>.
- 512 (20) McCleary, B. V.; DeVries, J. W.; Rader, J. I.; Cohen, G.; Prosky, L.; Mugford, D. C.;
513 Champ, M.; Okuma, K. Determination of Insoluble, Soluble, and Total Dietary Fiber
514 (CODEX Definition) by Enzymatic-Gravimetric Method and Liquid Chromatography:
515 Collaborative Study. *J. AOAC Int.* **2012**, *95* (3), 824–844.
516 https://doi.org/10.5740/jaoacint.CS2011_25.
- 517 (21) Talamond, P.; Doubeau, S.; Rochette, I.; Guyot, J.-P.; Treche, S. Anion-Exchange High-
518 Performance Liquid Chromatography with Conductivity Detection for the Analysis of
519 Phytic Acid in Food. *J. Chromatogr. A* **2000**, *871* (1–2), 7–12.
520 [https://doi.org/10.1016/S0021-9673\(99\)01226-1](https://doi.org/10.1016/S0021-9673(99)01226-1).
- 521 (22) Flory, P. J. *Principles of Polymer Chemistry*; Cornell University Press: Ithaca, New
522 York, 1953.
- 523 (23) Imai, T.; Kinoshita, M.; Hirata, F. Theoretical Study for Partial Molar Volume of Amino
524 Acids in Aqueous Solution: Implication of Ideal Fluctuation Volume. *J. Chem. Phys.*
525 **2000**, *112* (21), 9469–9478. <https://doi.org/10.1063/1.481565>.

- 526 (24) Fischer, H.; Polikarpov, I.; Craievich, A. F. Average Protein Density Is a Molecular-
527 Weight-Dependent Function. *Protein Sci.* **2009**, *13* (10), 2825–2828.
528 <https://doi.org/10.1110/ps.04688204>.
- 529 (25) Ma, C.-Y.; Harwalkar, V. R. Studies of Thermal Denaturation of Oat Globulin by
530 Differential Scanning Calorimetry. *J. Food Sci.* **1988**, *53* (2), 531–534.
531 <https://doi.org/10.1111/j.1365-2621.1988.tb07749.x>.
- 532 (26) Boye, J.; Zare, F.; Pletch, A. Pulse Proteins: Processing, Characterization, Functional
533 Properties and Applications in Food and Feed. *Food Res. Int.* **2010**, *43* (2), 414–431.
534 <https://doi.org/10.1016/j.foodres.2009.09.003>.
- 535 (27) Tyler, R. T.; Youngs, C. G.; Sosulski, F. W. Air Classification of Legumes. I. Separation
536 Efficiency, Yield, and Composition of the Starch and Protein Fractions. *Cereal Chem.*
537 **1981**, *58*, 144–148.
- 538 (28) Pelgrom, P. J. M.; Wang, J.; Boom, R. M.; Schutyser, M. A. I. Pre- and Post-Treatment
539 Enhance the Protein Enrichment from Milling and Air Classification of Legumes. *J.*
540 *Food Eng.* **2015**, *155*, 53–61. <https://doi.org/10.1016/j.jfoodeng.2015.01.005>.
- 541 (29) Ricci, L.; Umiltà, E.; Righetti, M. C.; Messina, T.; Zurlini, C.; Montanari, A.; Bronco,
542 S.; Bertoldo, M. On the Thermal Behavior of Protein Isolated from Different Legumes
543 Investigated by DSC and TGA. *J. Sci. Food Agric.* **2018**, *98* (14), 5368–5377.
544 <https://doi.org/10.1002/jsfa.9078>.
- 545 (30) Eliasson, A.-C. Differential Scanning Calorimetry Studies on Wheat Starch—Gluten
546 Mixtures. *J. Cereal Sci.* **1983**, *1* (3), 199–205. [https://doi.org/10.1016/S0733-5210\(83\)80021-6](https://doi.org/10.1016/S0733-5210(83)80021-6).
- 548 (31) Marsano, E.; Corsini, P.; Canetti, M.; Freddi, G. Regenerated Cellulose-Silk Fibroin
549 Blends Fibers. *Int. J. Biol. Macromol.* **2008**, *43* (2), 106–114.
550 <https://doi.org/10.1016/j.ijbiomac.2008.03.009>.
- 551 (32) Derbyshire, E.; Wright, D. J.; Boulter, D. Legumin and Vicilin, Storage Proteins of
552 Legume Seeds. *Phytochemistry* **1976**, *15* (1), 3–24. [https://doi.org/10.1016/S0031-9422\(00\)89046-9](https://doi.org/10.1016/S0031-9422(00)89046-9).
- 554 (33) Danielsson, C. E. Seed Globulins of the Gramineae and Leguminosae. *Biochem. J.* **1949**,
555 *44* (4), 387–400. <https://doi.org/10.1042/bj0440387>.
- 556 (34) Osborne, T. B.; Campbell, G. F. The Proteids of the Pea, Lentil, Horse Bean, and Vetch.
557 *J. Am. Chem. Soc.* **1898**, *20* (6), 410–419. <https://doi.org/10.1021/ja02068a003>.
- 558 (35) Sirtori, E.; Isak, I.; Resta, D.; Boschin, G.; Arnoldi, A. Mechanical and Thermal
559 Processing Effects on Protein Integrity and Peptide Fingerprint of Pea Protein Isolate.
560 *Food Chem.* **2012**, *134* (1), 113–121. <https://doi.org/10.1016/j.foodchem.2012.02.073>.
- 561 (36) Barbana, C.; Boye, J. I. In Vitro Protein Digestibility and Physico-Chemical Properties
562 of Flours and Protein Concentrates from Two Varieties of Lentil (*Lens Culinaris*). *Food*
563 *Funct* **2013**, *4* (2), 310–321. <https://doi.org/10.1039/C2FO30204G>.

- 564 (37) Chang, L.; Lan, Y.; Bandillo, N.; Ohm, J.-B.; Chen, B.; Rao, J. Plant Proteins from Green
565 Pea and Chickpea: Extraction, Fractionation, Structural Characterization and Functional
566 Properties. *Food Hydrocoll.* **2022**, *123*, 107165.
567 <https://doi.org/10.1016/j.foodhyd.2021.107165>.
- 568 (38) Singh, D. K.; Rao, A. S.; Singh, R.; Jambunathan, R. Amino Acid Composition of
569 Storage Proteins of a Promising Chickpea (*Cicer Arietinum* L) Cultivar. *J. Sci. Food*
570 *Agric.* **1988**, *43* (4), 373–379. <https://doi.org/10.1002/jsfa.2740430410>.
- 571 (39) Tavano, O. L.; Neves, V. A. Isolation, Solubility and in Vitro Hydrolysis of Chickpea
572 Vicilin-like Protein. *LWT - Food Sci. Technol.* **2008**, *41* (7), 1244–1251.
573 <https://doi.org/10.1016/j.lwt.2007.08.003>.
- 574 (40) Yin, S.-W.; Tang, C.-H.; Yang, X.-Q.; Wen, Q.-B. Conformational Study of Red Kidney
575 Bean (*Phaseolus Vulgaris* L.) Protein Isolate (KPI) by Tryptophan Fluorescence and
576 Differential Scanning Calorimetry. *J. Agric. Food Chem.* **2011**, *59* (1), 241–248.
577 <https://doi.org/10.1021/jf1027608>.
- 578 (41) Gupta, R.; Dhillon, S. Characterization of Seed Storage Proteins of Lentil (*Lens Culinaris*
579 M.). *Ann. Biol.* **1993**, *9*, 71–78.
- 580 (42) Cruz-Orea, A.; Pitsi, G.; Jamée, P.; Thoen, J. Phase Transitions in the Starch–Water
581 System Studied by Adiabatic Scanning Calorimetry. *J. Agric. Food Chem.* **2002**, *50* (6),
582 1335–1344. <https://doi.org/10.1021/jf0110396>.
- 583 (43) Habeych, E.; Guo, X.; van Soest, J.; van der Goot, A. J.; Boom, R. On the Applicability
584 of Flory–Huggins Theory to Ternary Starch–Water–Solute Systems. *Carbohydr. Polym.*
585 **2009**, *77* (4), 703–712. <https://doi.org/10.1016/j.carbpol.2009.02.012>.
- 586 (44) van der Sman, R. G. M.; Meinders, M. B. J. Prediction of the State Diagram of Starch
587 Water Mixtures Using the Flory–Huggins Free Volume Theory. *Soft Matter* **2011**, *7* (2),
588 429–442. <https://doi.org/10.1039/C0SM00280A>.
- 589 (45) Joshi, M.; Adhikari, B.; Aldred, P.; Panozzo, J. F.; Kasapis, S. Physicochemical and
590 Functional Properties of Lentil Protein Isolates Prepared by Different Drying Methods.
591 *Food Chem.* **2011**, *129* (4), 1513–1522.
592 <https://doi.org/10.1016/j.foodchem.2011.05.131>.
- 593 (46) Kaur, M.; Singh, N. Characterization of Protein Isolates from Different Indian Chickpea
594 (*Cicer Arietinum* L.) Cultivars. *Food Chem.* **2007**, *102* (1), 366–374.
595 <https://doi.org/10.1016/j.foodchem.2006.05.029>.
- 596 (47) Papalamprou, E. M.; Doxastakis, G. I.; Biliaderis, C. G.; Kiosseoglou, V. Influence of
597 Preparation Methods on Physicochemical and Gelation Properties of Chickpea Protein
598 Isolates. *Food Hydrocoll.* **2009**, *23* (2), 337–343.
599 <https://doi.org/10.1016/j.foodhyd.2008.03.006>.
- 600 (48) Paredes-López, O.; Ordorica-Falomir, C.; Olivares-Vázquez, M. R. Chickpea Protein
601 Isolates: Physicochemical, Functional and Nutritional Characterization. *J. Food Sci.*
602 **1991**, *56* (3), 726–729. <https://doi.org/10.1111/j.1365-2621.1991.tb05367.x>.

603 (49) Law, H.-Y.; Choi, S.-M.; Ma, C.-Y. Study of Conformation of Vicilin from Dolichos
604 Lablab and Phaseolus Calcaratus by Fourier-Transform Infrared Spectroscopy and
605 Differential Scanning Calorimetry. *Food Res. Int.* **2008**, *41* (7), 720–729.
606 <https://doi.org/10.1016/j.foodres.2008.05.004>.

607 (50) Tang, C.-H.; Ma, C.-Y. Heat-Induced Modifications in the Functional and Structural
608 Properties of Vicilin-Rich Protein Isolate from Kidney (Phaseolus Vulgaris L.) Bean.
609 *Food Chem.* **2009**, *115* (3), 859–866. <https://doi.org/10.1016/j.foodchem.2008.12.104>.

610

611

612 **Figure captions**

613 **Fig. 1.** DSC thermograms of lentil, chickpea and bean protein-enriched fractions for water
614 contents $X = 0.4 \text{ kg kg}^{-1} \text{ db}$ (a), $X = 1.0 \text{ kg kg}^{-1} \text{ db}$ (b) and $X = 2.0 \text{ kg kg}^{-1} \text{ db}$ (c). The
615 experimental dimensionless heat flows (dots) were modeled using the overall procedure
616 described in Lefèvre *et al.*¹³ The predicted dimensionless heat flows and P1 and P2 endotherms
617 are represented by the solid, dashed, and dotted lines, respectively. RMSE were calculated
618 between experimental and predicted heat flows for the different water contents.

619 **Fig. 2.** Parameters of the Gaussian functions T_i (a,b), ΔT_i (c,d) and β_{P1} (e) represented as a
620 function of water volume fraction (ϕ) or water content (X) in the water-protein mixture for the
621 lentil, chickpea and bean protein-enriched fractions. Dots represent the primary parameters of
622 the Gaussian function obtained using the desummation method by fitting the experimental
623 dimensionless heat flows to Eq. (1) for each water content. The solid lines represent the
624 modeling of the Gaussian parameters using the overall identification procedure for every water
625 contents in the same fitting session.

626 **Fig. 3.** DSC thermograms of protein-enriched fractions of lentils (a), chickpeas (b) and beans
627 (c) using the double scan procedure, for $X = 0.8 \text{ kg kg}^{-1} \text{ db}$. Samples were pre-heated from
628 $20 \text{ }^\circ\text{C}$ to $80 \text{ }^\circ\text{C}$, $110 \text{ }^\circ\text{C}$ or $160 \text{ }^\circ\text{C}$ followed by standard heating from $20 \text{ }^\circ\text{C}$ to $160 \text{ }^\circ\text{C}$. A control
629 sample (only standard heating from $20 \text{ }^\circ\text{C}$ to $160 \text{ }^\circ\text{C}$) is presented for the sake of comparison.

630 **Fig. 4.** Modeled denaturation diagram of lentil, chickpea and bean proteins obtained with the
631 desummation procedure. Isovalue lines showing the degree of protein denaturation (unfolding
632 and aggregation coupled) are presented in a temperature T versus water content X diagram.

633

Tables

Table 1. Experimental conditions of the database according to the type of pulse: water content (X) of protein samples analyzed with DSC from 20 °C to 160 °C.

X (kg kg ⁻¹ db)	Lentil	Chickpea	Bean
0.2	nd	nd	×
0.3	×	nd	–
0.4	×	×	×
0.6	×	×	×
0.8	×	×	×
1.0	×	×	×
1.2	–	×	×
1.4	–	×	×
1.6	–	×	×
1.8	–	×	×
2.0	×	×	×
2.2	–	–	–
2.4	–	–	–
2.5	–	×	×
2.6	–	–	–
2.8	–	–	–
3.0	×	×	×
3.5	×	–	×
4.0	×	–	–
Total measurements	18	22	26

×: measured in duplicate.

nd: incomplete signal detected by DSC at $T \leq 160$ °C;

–: not tested.

Table 2. Chemical composition of protein-enriched fractions as a fine fraction obtained after dry fractionation and air classification (g/100g dry weight basis)

Pulse	Moisture	Starch	Proteins	IDF	SDF	Lipids	Phytates	Alpha-galactosides
Lentil	7.9 ± 0.1	3.0 ± 0.6	55.8 ± 0.1	11.1 ± 1.4	3.1 ± 0.6	2.2 ± 0.1	3.5 ± 0.1	6.3 ± 0.5
Chickpea	5.3 ± 0.1	5.6 ± 0.7	38.2 ± 1.5	18.5 ± 1.1	2.7 ± 0.8	11.5 ± 0.1	2.2 ± 0.1	5.2 ± 0.8
Bean	5.8 ± 0.1	4.2 ± 0.3	49.4 ± 0.1	13.9 ± 3.1	3.7 ± 1.4	2.7 ± 0.2	2.8 ± 0.1	6.3 ± 0.1

IDF: insoluble dietary fibers; SDF: soluble dietary fibers

Table 3. Parameters of Eqs. (3), (5) and (6) used to describe the heat flows (Eq. (1)) for lentil, chickpea and bean protein-enriched samples (mean

values \pm 95 % confidence interval). The values were used to calculate the degree of protein denaturation $\tau = \sum_{i=P1, P2} \beta_i \times \frac{1}{2} \left(1 + \operatorname{erf} \left(\frac{T - T_i}{\Delta T_i \sqrt{2}} \right) \right)$ with

two peaks (P1 and P2 for lentil and chickpea) or one peak (P1, bean).

Protein-enriched sample	$\frac{1}{T_i} - \frac{1}{T_{i,0}} = \frac{R}{\Delta h_{i,0}} \frac{v_g}{v_w} (\phi - \chi_i \phi^2)$						$\Delta T_i = \Delta T_{i,\infty} + (\Delta T_{i,0} - \Delta T_{i,\infty}) \exp\left(-\frac{X}{\gamma_i}\right)$					$\beta_{P1} = \beta_{P1,\infty} + (\beta_{P1,0} - \beta_{P1,\infty}) \exp(-X)$	
	$T_{P1,0}$ (°C)	$T_{P2,0}$ (°C)	$\Delta h_{P1,0}$ (kJ mol ⁻¹)	$\Delta h_{P2,0}$ (kJ mol ⁻¹)	χ_{P1}	χ_{P2}	$\Delta T_{P1,0}$ (°C)	$\Delta T_{P2,0}$ (°C)	$\Delta T_{P1,\infty}$ (°C)	$\Delta T_{P2,\infty}$ (°C)	γ_{P2}	$\beta_{P1,0}$	$\beta_{P1,\infty}$
Lentil	165.2 \pm 0.4	201.1 \pm 3.3	57.6 \pm 0.4	45.1 \pm 2.9	0.00 \pm 0.05	0.05 \pm 0.05	4.2 \pm 0.1	4.0 \pm 0.2	4.2 \pm 0.1	4.0 \pm 0.2	1	0.65 \pm 0.01	0.65 \pm 0.01
Chickpea	198.1 \pm 8.5	224.7 \pm 4.6	41.2 \pm 5.2	41.9 \pm 2.5	0.12 \pm 0.05	0.14 \pm 0.03	6.5 \pm 0.3	7.0 \pm 1.6	2.2 \pm 0.2	3.9 \pm 0.1	0.3 \pm 0.1	0.59 \pm 0.02	0.12 \pm 0.01
Bean	166.2 \pm 0.3		65.8 \pm 0.3		0.00 \pm 0.05		3.5 \pm 0.1		3.5 \pm 0.1			1	1

ϕ : volume fraction of water (m³ m⁻³)

X : water content (kg kg⁻¹ db)

γ_{P1} was fixed at 1.

$\beta_{P2} = 1 - \beta_{P1}$

Figures

Fig. 1.

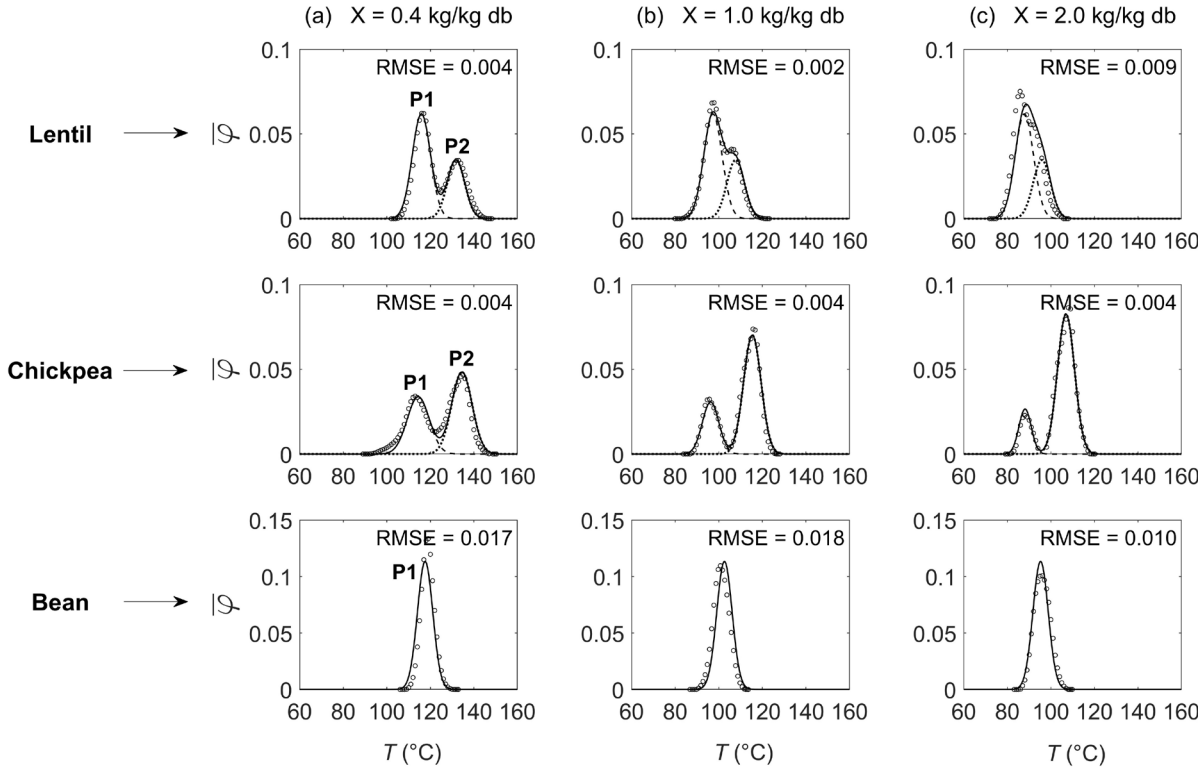


Fig. 2.

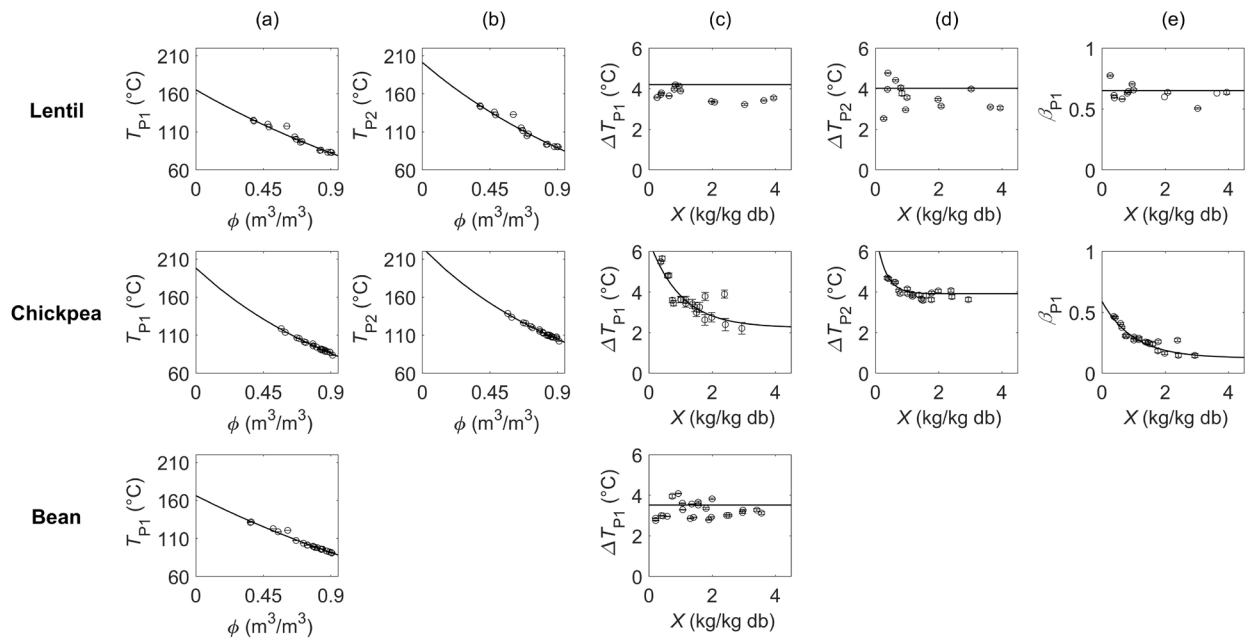


Fig. 3.

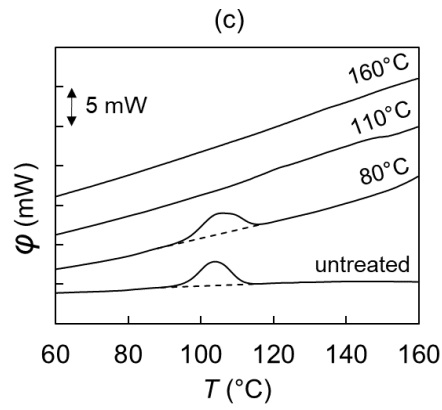
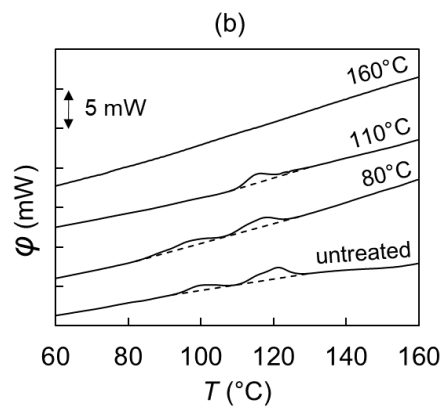
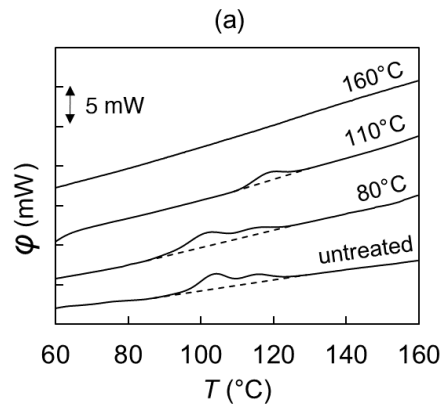
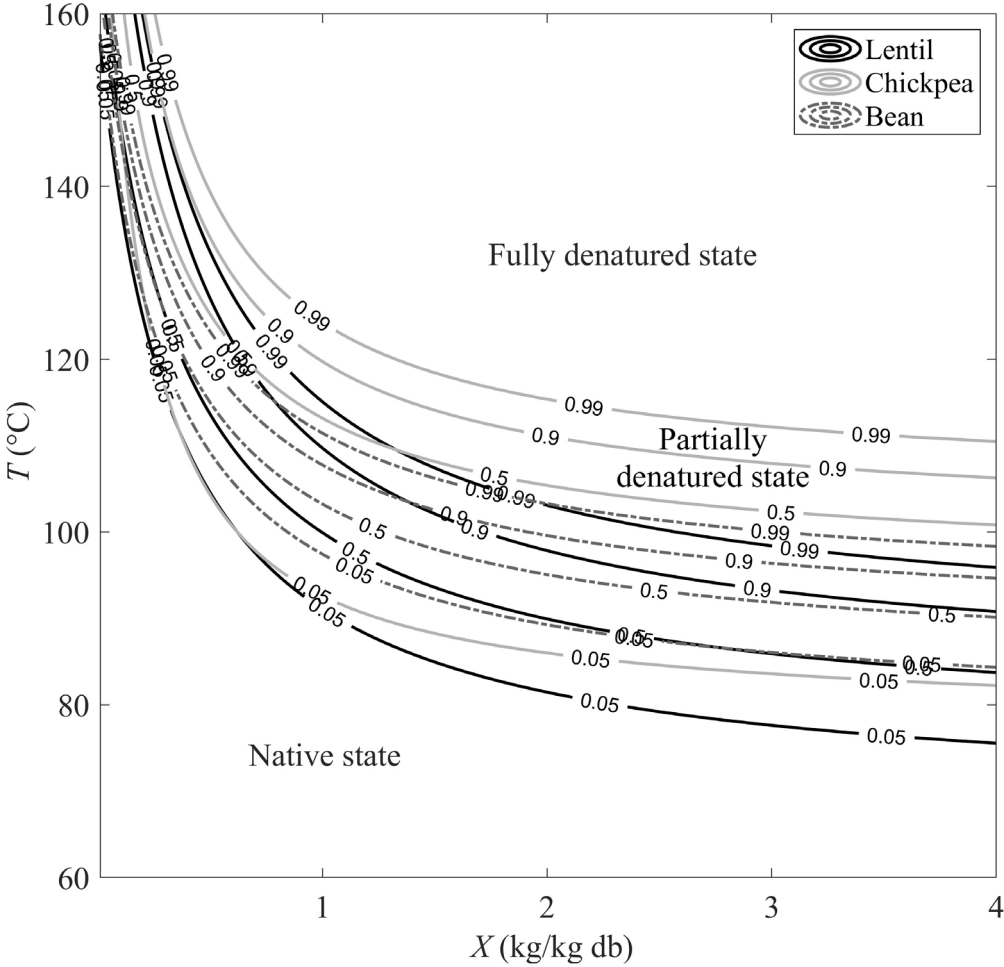
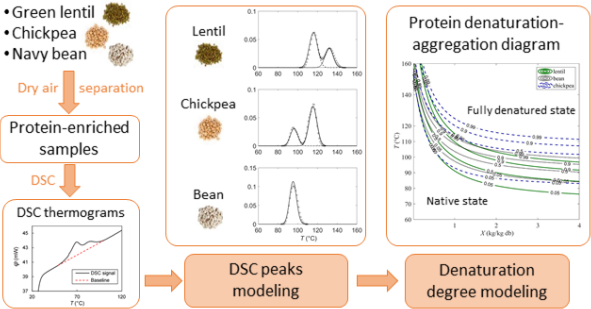


Fig. 4.



Graphic for Table of Contents



Label : For Table of Contents Only